Fracture, aggregation and segregation in dry, granular flows

James T. Jenkins[1] *and Michele* Larcher[2]

[1]Cornell University, Ithaca, NY, 14853, USA
[2]Free University of Bozen-Bolzano, I-39100, Bozen-Bolzano, Italy

Abstract. Particle fracture, the formation of small particles as the result of the breakage of large ones, and aggregation, the formation of large particles as the result of the combination of small ones, have important implications in industry (e.g. food processing, pharmaceutical production) and geophysics (e.g., snow avalanches and rock debris flows). Also, the presence of particles of different size that result from fracture and aggregation can induce segregation, resulting in the migration of large and small particles to different regions of the flow. Here, we formulate simple models for fracture and agglomeration and analyze the evolution of measures of the relative concentration of two sizes of spheres due the combined effects of fracture, aggregation, and segregation in dense, dry, granular flows. Particle breakage and combination is influenced by the frequency of collisions, by the local number density of the spheres, and by the particle kinetic energy. Segregation is predicted using a kinetic theory proposed by Larcher & Jenkins [2].

1 Introduction

We consider a steady, dense, dry, collisional flow [1] of a binary mixture of two types of inelastic spheres down an incline at an angle θ, under the influence of gravitational acceleration g. In earlier work, Larcher & Jenkins [2] predicted the evolution of concentration profiles in such flows using a theory for segregation appropriate for particles with relatively small differences in size and mass. In treating the evolution, they assume that the flow of the mixture reaches a fully-developed state much more rapidly than the concentrations of the two species. Here, we consider a similar situation, but allow for the possibility that depending on the particle kinetic energy and the frequency of collisions, a large sphere may fracture into two smaller spheres and two small spheres may aggregate into one larger sphere, in such a way that mass is conserved.

The two types of spheres, A and B, interact in collisions that are characterized by coefficients of normal restitution e and sliding friction μ. The spheres have different radii, r_A and r_B, with $r_{AB} = r_A + r_B$, masses, m_A and m_B, with $m_{AB} = m_A + m_B$, number densities, n_A and n_B, with $n = n_A + n_B$, and mass densities, $\rho_A = m_A n_A$ and $\rho_B = m_B n_B$, with $\rho = \rho_A + \rho_A$. The concentrations that correspond to the number densities are $c_A = 4\pi n_A r_A^3/3$, $c_B = 4\pi n_B r_B^3/3$ and $c = c_A + c_B$. When fracture and aggregation conserve mass, $r_A / r_B = (2\rho_B / \rho_A)^{1/3}$; so, for example, if the spheres are made of the same material, and A is the larger, the ratio of the radii of large to small spheres is $2^{1/3}$.

The local difference in the presence of the two types of spheres is described by means of the number density difference, $X \equiv (n_A - n_B) / 2n$, the kinetic energy T of the velocity fluctuations of the mixture is equal to half the average mass of the two types of spheres times one-third the mean of the square of their magnitude, and the average flow velocity is denoted by u. The coordinates x and y are along and transverse to the flow, with the origin of the y-axis at the base of the flow.

The frequency of collisions per unit sphere of large and small spheres are assumed to be identical and to coincide with frequency of collisions, ω, of a mixture of homogeneous spheres with radius r_{AB} ad mass m_{AB}.

$$\omega = \frac{24}{\pi^{1/2}} \frac{G}{r_{AB}} \left(\frac{2T}{m_{AB}} \right)^{1/2}, \tag{1}$$

where

$$G = 5.69c \frac{c_c - 0.49}{c_c - c}, \tag{2}$$

where c_c is a critical concentration given by $c_c = 0.58 + (0.64 - 0.58)\exp(-4.5\mu)$ [3].

2 Particle fracture

The number of large sphere collisions per unit volume can be evaluated as the product of the frequency of collisions per unit sphere referred to the mixture, given by Eq. (1), and the number density of species A, n_A, as

$$n_A \omega = n_A \frac{24}{\pi^{1/2}} \frac{G}{r_{AB}} \left(\frac{2T}{m_{AB}} \right)^{1/2}. \tag{3}$$

We assume that in some fraction, f_A, of collisions between two large spheres, they fracture into four small spheres. Then, the local rate of change of large

A video is available at https://doi.org/10.48448/ty5y-ev04

spheres per unit volume in a steady flow in the x-direction is

$$\frac{dn_A}{dt} = u\frac{dn_A}{dx} = -2n_A\omega f_A; \tag{4}$$

while the local change of small spheres per unit volume is

$$\frac{dn_B}{dt} = u\frac{dn_B}{dx} = 4n_A\omega f_A. \tag{5}$$

Eqs. (4) and (5) permit the determination of the evolution of the measure, X, of number density difference with time:

$$\begin{aligned}\frac{dX}{dt} &= u\frac{dX}{dx} \\ &= \frac{1}{2n}\left[\frac{dn_A}{dt} - \frac{dn_B}{dt} - \frac{n_A - n_B}{n}\left(\frac{dn_A}{dt} + \frac{dn_B}{dt}\right)\right] \\ &= -\frac{n_A}{n}\omega f_A\left(3+2X\right).\end{aligned} \tag{6}$$

Using the definition $X \equiv (n_A - n_B) / 2n$, n_A/n may be written in terms of X, and Eq. (6) becomes

$$\frac{dX}{dt} = u\frac{dX}{dx} = -\frac{1}{2}\omega f_A\left(1+2X\right)\left(3+2X\right). \tag{7}$$

3 Particle aggregation

With the frequency of collisions per unit sphere, ω, for the small spheres given by Eq. (1), the number of small sphere collisions per unit volume is

$$n_B\omega = n_B\frac{24}{\pi^{1/2}}\frac{G}{r_{AB}}\left(\frac{2T}{m_{AB}}\right)^{1/2}. \tag{8}$$

We assume that in some fraction, f_B, of collisions between two small spheres, they combine into one large sphere. Then, the local rate of change of small spheres per unit volume is

$$\frac{dn_B}{dt} = u\frac{dn_B}{dx} = -2n_B\omega f_B, \tag{9}$$

i.e., two small spheres are lost and a large sphere is gained. Similarly, the local rate of change of large spheres is

$$\frac{dn_A}{dt} = u\frac{dn_A}{dx} = n_A\omega f_A. \tag{10}$$

In the same way as for particle fracture, Eqs. (9) and (10) permit the determination of the evolution of X due to aggregation:

$$\frac{dX}{dt} = u\frac{dX}{dx} = \frac{1}{4}\omega f_B\left(1-2X\right)\left(3+2X\right). \tag{11}$$

4 Particle segregation

Larcher & Jenkins [2] characterize the segregation of two types of spheres using X, and show that when the differences $\delta r = (r_A / r_B) - 1$ and $\delta m = (m_A - m_B) / m_{AB}$ in radii and masses are small, the evolution of the segregation in uniform, inclined flow is governed by a mass balance:

$$\rho\frac{\partial X}{\partial t} + \frac{\partial}{\partial y}\left[\frac{m_A n}{4}\left(1-4X^2\right)\left(\tilde{v}_A - \tilde{v}_B\right)\right] = 0, \tag{12}$$

and a weighted difference in momentum balances for each type of sphere:

$$\begin{aligned}\tilde{v}_A - \tilde{v}_B = -D_{AB}\Bigg[&\left(\Gamma_1\delta m + R_1\delta r\right)\frac{1}{T}\frac{\partial T}{\partial y} \\ &+(\Gamma_2\delta m + R_2\delta r)\frac{m_{AB}g\cos\theta}{2T} + \frac{4}{1-4X^2}\frac{\partial X}{\partial y}\Bigg],\end{aligned} \tag{13}$$

where

$$D_{AB} \equiv \frac{\pi^{1/2}r_{AB}}{16G}\left(\frac{2T}{m_{AB}}\right)^{1/2}, \tag{14}$$

in which, in first approximation,

$$G = G_0 = 5.69c\frac{0.64-0.49}{0.64-c} \tag{15}$$

for frictionless spheres [3], and

$$\Gamma_1 = \frac{179}{29}G + \frac{105}{116} \doteq 6.17G, \tag{16}$$

$$\Gamma_2 = 2, \tag{17}$$

$$\begin{aligned}R_1 = \frac{5}{58}\left[2 + \frac{c\left(3-c\right)}{2-c} - \frac{12}{5}G\right] + 2G\left[3 + \frac{c\left(3-c\right)}{2-c}\right] \\ -\frac{12cH\left(1+4G\right)}{1+4G+4cH} \doteq -4.35G,\end{aligned} \tag{18}$$

and

$$R_2 = \frac{12cH}{1+4G+4cH} \doteq -3. \tag{19}$$

Equations (12) and (13) lead to an equation for the evolution of X [2]:

$$\frac{dX}{dt} = u\frac{dX}{dx}$$
$$= \frac{m_A}{2m_{AB}}\frac{\partial}{\partial y}\left\{\left(1-4X^2\right)D_{AB}\left[\left(\Gamma_1\delta m + R_1\delta r\right)\frac{1}{T}\frac{\partial T}{\partial y}\right.\right. \quad (20)$$
$$\left.\left. +(\Gamma_2\delta m + R_2\delta r)\frac{m_{AB}g\cos\theta}{2T} + \frac{4}{1-4X^2}\frac{\partial X}{\partial y}\right]\right\}.$$

5 Fracture, aggregation, segregation

The descriptions of particle fracture, Eq. (7), aggregation, Eq. (11), and segregation, Eq. (20), can be combined with the frequency of collisions, Eq. (1), to obtain an expression for the change of X due to the three mechanisms:

$$\frac{dX}{dt} = u\frac{dX}{dx}$$
$$= \frac{m_A}{2m_{AB}}\frac{\partial}{\partial y}\left\{\left(1-4X^2\right)D_{AB}\left[\left(\Gamma_1\delta m + R_1\delta r\right)\frac{1}{T}\frac{\partial T}{\partial y}\right.\right.$$
$$\left.\left. +(\Gamma_2\delta m + R_2\delta r)\frac{m_{AB}g\cos\theta}{2T} + \frac{4}{1-4X^2}\frac{\partial X}{\partial y}\right]\right\}$$
$$-\frac{12}{\pi^{1/2}}\frac{G}{r_{AB}}\left(\frac{2T}{m_{AB}}\right)^{1/2}\left(3+2X\right)\left[f_A\left(1+2X\right) - \frac{1}{2}f_B\left(1-2X\right)\right]. \quad (21)$$

The expression for the granular temperature profile in Eq. (21) can be obtained from the component of the mixture momentum balance across the flow, under the hypothesis that the mixture concentration is constant [4]:

$$T = \frac{m_{AB}\left(h-y\right)}{4\left(1+\varepsilon\right)G}g\cos\theta, \quad (22)$$

where ε is an effective coefficient of restitution, given in terms e and μ by $\varepsilon = e-(3/2)\mu\exp(-3\mu)$. As a result of Eq. (22), $\partial T/\partial y = -T/(h-y)$.

The velocity profile for the mixture results from the mixture momentum balance along the flow and the relationship between the mixture shear stress and the mixture velocity gradient. These, upon integration and neglect of the slip velocity at the bed [4], give

$$u = \frac{5\pi^{1/2}}{6J}\frac{1}{r_{AB}}\left(\frac{1+\varepsilon}{2G}g\cos\theta\right)^{1/2}\left[h^{3/2} - \left(h-y\right)^{3/2}\right]\tan\theta. \quad (23)$$

The correction factor due to the presence of segregation [2] was neglected in Eqs. (22) and (23), consistently with the simplicity of the proposed model.

We make x and y dimensionless by r_{AB}, u dimensionless by $(gr_{AB})^{1/2}$, and T dimensionless by $m_{AB}r_{AB}g/2$. With this, Eq. (23) for the velocity, and Eq. (14) for the diffusion coefficient, Eq. (21) becomes

$$\frac{80}{3}\frac{m_{AB}}{m_A}\frac{1+\varepsilon}{J}G\left[h^{3/2} - \left(h-y\right)^{3/2}\right]\tan\theta\frac{dX}{dx}$$
$$= \frac{\partial}{\partial y}\left[\left(h-y\right)^{1/2}\left\{\left[2\left(1+\varepsilon\right)(\Gamma_2\delta m + R_2\delta r)G\right.\right.\right.$$
$$\left.\left.\left. -\left(\Gamma_1\delta m + R_1\delta r\right)\right]\frac{1-4X^2}{h-y} + 4\frac{\partial X}{\partial y}\right\}\right]$$
$$-\frac{384}{\pi}\frac{m_{AB}}{m_A}G^2\left(h-y\right)^{1/2}\left(3+2X\right)\left[f_A\left(1+2X\right) - \frac{1}{2}f_B\left(1-2X\right)\right]. \quad (24)$$

When lengths are normalized by the flow depth and $z = y/h$ and $\ell = x/h$, Eq. (24) becomes

$$\frac{80}{3}\frac{m_{AB}}{m_A}\frac{1+e}{J}G\left[1-\left(1-z\right)^{3/2}\right]\tan\theta\frac{dX}{d\ell}$$
$$= \frac{1}{h^2}\frac{\partial}{\partial z}\left[\left(1-z\right)^{1/2}\left\{\left[2\left(1+\varepsilon\right)(\Gamma_2\delta m + R_2\delta r)G\right.\right.\right.$$
$$\left.\left.\left. -\left(\Gamma_1\delta m + R_1\delta r\right)\right]\frac{1-4X^2}{1-z} + 4\frac{\partial X}{\partial z}\right\}\right]$$
$$-\frac{384}{\pi}\frac{m_{AB}}{m_A}G^2\left(1-z\right)^{1/2}\left(3+2X\right)\left[f_A\left(1+2X\right) - \frac{1}{2}f_B\left(1-2X\right)\right]. \quad (25)$$

Using the approximations given in Eqs. (16), (17), (18) and (19), and with $m_{AB}/m_A = 3/2$, Eq. (25) can be simplified further to

$$40\frac{1+e}{J}G\left[1-\left(1-z\right)^{3/2}\right]\tan\theta\frac{dX}{d\ell}$$
$$= \frac{1}{h^2}\frac{\partial}{\partial z}\left[\left(1-z\right)^{1/2}\left\{\left[2\left(1+\varepsilon\right)(2\delta m - 3\delta r)G\right.\right.\right.$$
$$\left.\left.\left. -\left(6.2\delta m - 4.4\delta r\right)\right]\frac{1-4X^2}{1-z} + 4\frac{\partial X}{\partial z}\right\}\right]$$
$$-\frac{576}{\pi}G^2\left(1-z\right)^{1/2}\left(3+2X\right)\left[f_A\left(1+2X\right) - \frac{1}{2}f_B\left(1-2X\right)\right]. \quad (26)$$

6 An example

In Fig. 1, we show evolving profiles generated using the Matlab code *pdepe.m* for the measure, X, of number density difference of spheres made of the same material for three different situations: the first is for segregation without fracture or aggregation; the second in for segregation with fracture, but no aggregation; and the third is for segregation with fracture and aggregation occurring at different rates. As for pure segregation, the flow of the mixture was assumed to remain steady as the individual particle concentrations evolved.

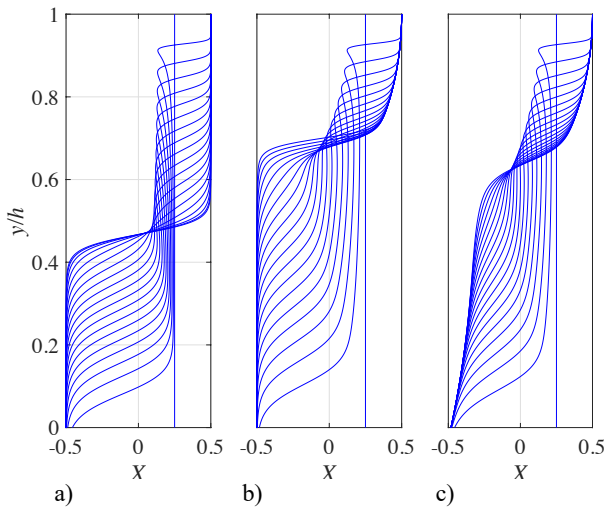

Fig. 1. The evolution of profiles of X for a) segregation alone, $f_A = f_B = 0$; b) segregation with fracture but no aggregation, $f_A = 10^{-6}$ and $f_B = 0$; and c) segregation with fracture and aggregation, $f_A = 10^{-6}$ and $f_B = 5\text{x}10^{-7}$. The particle properties are $\rho_A/\rho_B = 1.0$, $r_A/r_B = 2^{1/3}$, $e = 0.85$, and $\mu = 0.20$. The dense, inclined flow is at a non-dimensional depth $h/r_{AB} = 20$ and an inclination of $\theta = 25^\circ$. The curves are drawn at intervals of 50 dimensionless depths, from an initiation at a value of $X = 0.25$ throughout the bed, until a distance of 1000 dimensionless depths.

In the figure, we consider a rather long distance of evolution, because segregation is slow and we want to show it being almost complete. Because the strength of the diffusion, Eq. (14), is proportional to $T^{1/2}$, which, by Eq. (23), is proportional to the shear rate u', segregation takes place more rapidly where the temperature and shear rate are greatest [5]. Eqs. (3) and (8) show that this is also true of the fracture and the aggregation. Because the granular temperature decreases from the bottom to the top of the flow, the evolution of segregation, fracture, and aggregation is more rapid near the bottom than at the top.

As indicated in Fig. 1a), the larger spheres migrate to the cooler regions of the flow [4]. Fracture increases the number of small spheres in relation to the number of large spheres. This accounts for the difference between the final states of Figs. 1a) and 1b). Fracture and aggregation also influence the evolution of the difference in local number fractions, X, through the last term in Eq. (26). Creation of more smaller spheres speeds the evolution of X, while creation of more larger spheres slows its evolution. This effect is seen in the difference in the evolution of X between Figs. 1a) and 1b) and in the difference in its evolution between Figs. 1b) and 1c). That is, the evolution towards a fully-developed state in Fig. 1c) is far slower than that in Fig. 1b), because of the creation of larger spheres through aggregation near the bottom of the flow.

7 Conclusion

We have proposed a simple model for describing the time-evolution of particle breakage, aggregation and segregation and possible combinations of the three mechanisms. Breakage and aggregation depend on the frequency and intensity of collisions, while segregation is predicted through kinetic theory.

The model is an oversimplification in that it makes the unrealistic assumptions that a large sphere fractures into two small spheres, and that two small spheres aggregate into a single large sphere; but these assumptions permit the expression for the frequency of collision for the mixture to be employed to describe the rates of fracture and aggregation. In any case, we believe that the simplicity of the model is a virtue and that the model retains sufficient complexity and realism and to make it interesting and, possibly, predictive.

We plan to carry out discrete-element numerical simulations to test the model of segregation, fracture, and aggregation in the dense, inclined flow studied here.

References

[1] J.T. Jenkins, Gran. Matt. **10**, 47 (2007)

[2] M. Larcher and J.T. Jenkins, J. Fluid Mech. **782**, 405 (2015)

[3] D. Berzi and D. Vescovi, Phys. Fluids **27**, 013302 (2015)

[4] M. Larcher and J.T. Jenkins, Phys. Fluids **25**, 113301 (2013)

[5] R. Artoni, M. Larcher, J.T. Jenkins, P. Richard, Soft Matter **17**, 2596 (2021)